

# A super resolution metalens with phase compensation mechanism

Changbao Ma and Zhaowei Liu<sup>a)</sup>

Department of Electrical and Computer Engineering, University of California, San Diego, La Jolla, California 92093-0407, USA

(Received 1 January 2010; accepted 15 April 2010; published online 4 May 2010)

We propose a metalens consisting of a metamaterial slab that can support the propagation of waves with high wave vectors and a nonperiodic plasmonic waveguide coupler atop that can provide phase compensation and wave vector matching. The principle of the metalens is analyzed and numerically verified. We show that the metalens not only can achieve super resolution focusing but also has the fundamental properties of a conventional optical lens, such as Fourier transform and imaging. The proposed metalens may offer exceptional opportunities for optical system design and information processing. © 2010 American Institute of Physics. [doi:10.1063/1.3427199]

The lens is the most fundamental element in optics. A glass lens refracts and focuses light relying on curved interfaces, as is illustrated two-dimensionally (2D) using a plano-convex lens in Fig. 1(a). The focusing can also be achieved by a zone plate allowing only the in-phase light zones to pass and interfere, as shown in Fig. 1(b). However, their spatial resolution has long been believed to be limited to approximately half of the working wavelength.<sup>1</sup> Although the resolution can be improved by liquid or solid immersion techniques,<sup>2–4</sup> the enhancement is still limited by the refractive index of natural materials.<sup>4</sup> From the point of view of Fourier optics, such lateral resolution limit originates from the limited transverse wave vector ( $k$ -vector) of the propagating waves in the materials. Recently, various superlenses have emerged with resolving power beyond the diffraction limit.<sup>5–13</sup> However, such superlenses cannot focus a plane wave due to the lack of phase compensation mechanism. Here we propose a metalens based on metamaterials, which not only can achieve super resolution focusing through phase compensation, but also possesses a conventional optical lens' basic properties, such as Fourier transform and imaging.

To achieve higher resolution, a material that can support the propagation of light with higher  $k$ -vectors is needed. Metamaterials, which are artificially engineered nanocomposites that can provide extraordinary material properties beyond the natural availabilities,<sup>14–16</sup> become an incomparable candidate for this purpose. Because the light with high  $k$ -vectors inside a metamaterial cannot transmit to air due to total internal reflection, a bidirectional coupling mechanism to convert waves from high  $k$ -vectors in the metamaterial to low  $k$ -vectors in air and vice versa is needed. Instead of transforming the metamaterial into a cylindrical coordinate as in the hyperlens<sup>9–11</sup> or shaping the metamaterial

surface<sup>17,18</sup> or adding a surface diffractive element,<sup>12</sup> we introduce a planar plasmonic metal-insulator-metal (MIM) waveguide<sup>19–22</sup> coupler to fulfill this task. Therefore, we propose a “metalens” concept by combining a metamaterial slab and a plasmonic waveguide coupler (PWC) [see Fig. 1(c)].

The metalens concept requires that the metamaterial be able to support the propagation of waves with high  $k$ -vectors. For example, metamaterials with an applanate elliptic ( $\epsilon'_{xy} > 0, \epsilon'_z > 0$ ) or a hyperbolic ( $\epsilon'_{xy} > 0, \epsilon'_z < 0$ ) dispersion  $k_x^2/\epsilon_z + k_z^2/\epsilon_x = k_0^2$  shown in the inset of Fig. 1(c), which is represented in 2D for simplicity, satisfies this condition. Here  $k_0$  is the free space wave vector,  $\epsilon$ 's are the complex permittivity in their corresponding direction, and the prime denotes the real part. The material properties required for metalens analyzed above can be easily obtained using multilayer<sup>23</sup> and nanowire<sup>24</sup> metamaterials.

To make a focusing lens using the metamaterial with the required properties above, a phase compensation mechanism is needed. Due to the surface plasmonic waveguiding effect in an MIM waveguide,<sup>22</sup> a large range of propagation constants can be easily obtained, so a nonperiodically distributed PWC is ideal to tailor the phase of the light.<sup>19–21</sup> This is in contrast to the periodic grating used in the previously demonstrated far-field superlens,<sup>12</sup> which can only convert the evanescent waves to propagating waves, but cannot provide magnification because there is no consideration for phase compensation.

A 2D metalens and its phase compensation diagram is schematically shown in Fig. 1(c). The light from a line object inside the anisotropic metamaterial propagates with a specific wave front that is determined by the metamaterial properties. Waves spread out in space and are incident upon the

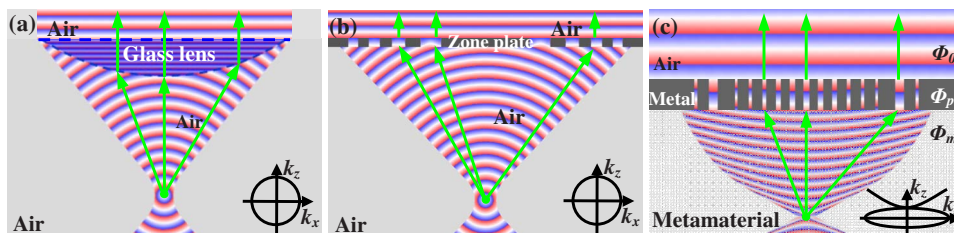


FIG. 1. (Color online) Geometry and principle of (a) a refractive glass lens, (b) a diffractive zone plate, and (c) a metalens. The inset at the lower right corner of each figure is its dispersion relation.

<sup>a)</sup>Electronic mail: zhaowei@ece.ucsd.edu.

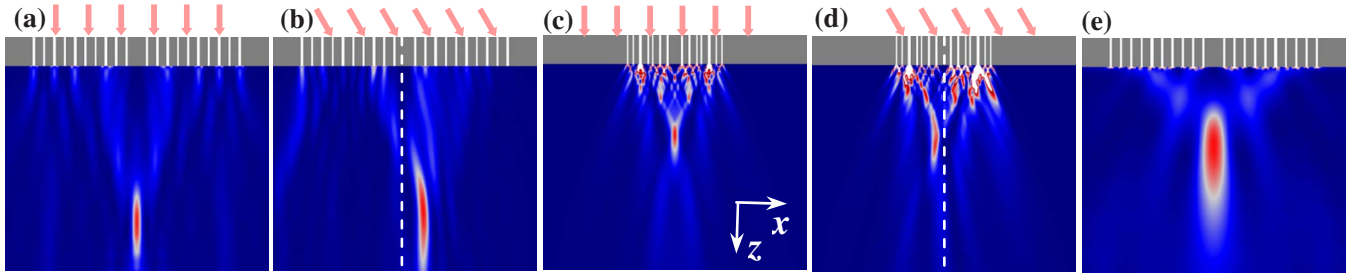


FIG. 2. (Color online) Deep subwavelength focusing and Fourier transform of the metalens. A metalens consisting of an Ag PWC and a metamaterial with an elliptic dispersion ( $\epsilon_x=3.4+0.05i$ ,  $\epsilon_z=11.3+0.9i$ ), achieving a 59 nm focus (FWHM) at the focal length  $f=1.0 \mu\text{m}$ , illuminated with (a) a normal and (b) a tilted plane wave. A metalens consisting of an Al PWC and a metamaterial with a hyperbolic dispersion ( $\epsilon_x=3.7+0.06i$ ,  $\epsilon_z=-8.9+1.8i$ ), achieving a 52 nm focus at  $f=0.5 \mu\text{m}$ , illuminated with (c) a normal and (d) a tilt plane wave. (e) An Ag waveguide plate in free space with a 181 nm focus at  $f=0.5 \mu\text{m}$ . Metalens dimensions:  $x=1.8 \mu\text{m}$ ,  $z=1.4 \mu\text{m}$ . PWC height: 200 nm. Slit widths: 10–20 nm. Material in slits: air.

MIM waveguides, with various lateral  $k$ -vectors and initial phases at different locations. All the waves that hit on the waveguides can excite the waveguide mode. The waveguides therefore need to be designed differently in terms of propagating constant, so that a nonflat wave front underneath the waveguide layer can be transformed to a flat one atop, and vice versa. As each waveguide and the spacing are in nanoscale, the top surface of the PWC can be regarded as a collection of point sources with a same phase. Based on the Huygens principle, a plane wave forms and continues to propagate in the free space above the PWC.

Because this principle is reciprocal, when a plane wave is incident on the metalens from the top, a deep subwavelength focus can be formed in the metamaterial through constructive interference. So the phase condition for focusing a plane wave by a metalens is  $\Phi_m + \Phi_p = \Phi_{\text{const}} + 2l\pi$ , with  $\Phi_m = [\epsilon'_x z^2 + \epsilon'_z x^2]^{1/2}$  being the phase change in the metamaterial slab,  $\Phi_p$  being the phase change introduced by each waveguide (assuming there is no coupling between waveguides),  $\Phi_{\text{const}}$  being a constant and  $l$  being an integer. The plasmonic MIM waveguides can be accordingly designed to have a different propagation constant  $\beta = \beta(\epsilon_m, \epsilon_d, w)$  in a wide range, thus providing the necessary phase compensation  $\Phi_p \sim \text{Re}(\beta h)$ .<sup>19–21</sup> Here  $\epsilon_m$  and  $\epsilon_d$  are the permittivity of the metal and insulator, respectively, and

$h$  is the height of the waveguide. Therefore, the phase compensation can be achieved by adjusting the geometric parameters ( $w, h$ ) and the material properties ( $\epsilon_m$  and  $\epsilon_d$ ) of the plasmonic waveguides, with  $w$  being the width of the waveguide. The planar example shown in Fig. 1(c) modulates the waveguide phase through  $w$  only.

To verify the metalens concept, simulations have been carried out at the wavelength of 365 nm. Note that all simulation plots are  $|E_x|^2$  profiles. Figure 2 shows the simulations of two metalenses that demonstrate their deep subwavelength focusing and Fourier transform functions. For comparison purpose, Fig. 2(e) shows the simulation of an Ag PWC in air with a diffraction-limited focal spot. With normal TM plane wave illumination, the metalens with an elliptically and a hyperbolically dispersive metamaterial shown in Figs. 2(a) and 2(c) achieved a deep subwavelength focal spot with an full width at half maximum (FWHM) of 59 nm and 52 nm, respectively. Comparing with the conventional lens in air, about threefold resolution enhancement has been demonstrated by the two examples. With tilted illumination, the focal spot of the metalens with the elliptic dispersion shifts accordingly along the incident direction, which is similar to a conventional optical lens, as shown in Fig. 2(b). On the contrary, the focal spot shifts to the opposite side when the metalens possesses a hyperbolic dispersion, as shown in Fig.

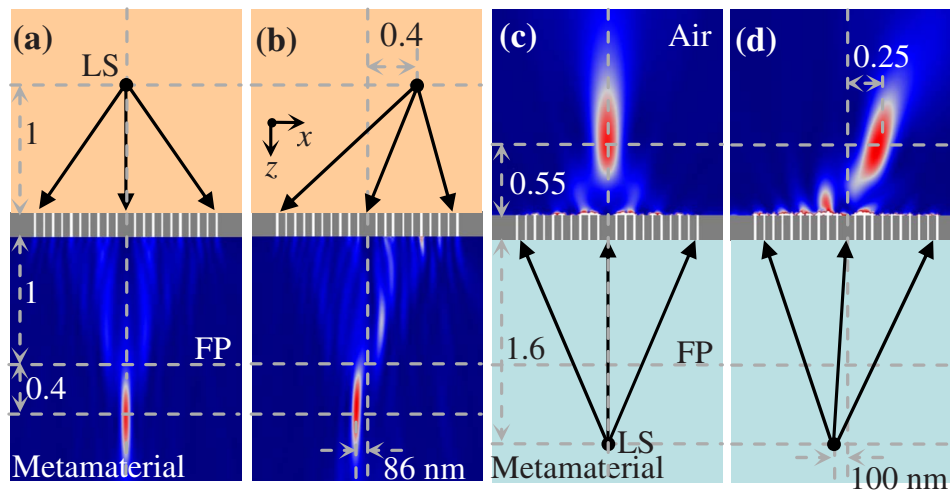


FIG. 3. (Color online) Imaging characteristics of a metalens. (a) A deep subwavelength scale image in the metamaterial is formed for an on-axis line source (LS) in air. (b) The image is shifted when the line source is off-axis in air, attaining a demagnification of 4.65. (c) A wavelength scale image in air is formed for an on-axis line source in the metamaterial. (d) The image is shifted when the line source is off-axis in the metamaterial, attaining a magnification of 2.5. Metamaterial properties: ( $\epsilon_x=3.4+0.05i$ ,  $\epsilon_z=11.3+0.9i$ ). Material in slits: air.  $f=1 \mu\text{m}$ . Simulated  $f_{\text{air}}=180 \text{ nm}$ . Figure dimensions:  $x=1.8 \mu\text{m}$  and  $z=3.7 \mu\text{m}$ . PWC height: 200 nm. Slit widths: 10–20 nm. When not specified, the unit of geometric parameters is  $\mu\text{m}$ . FP denotes focal plane.

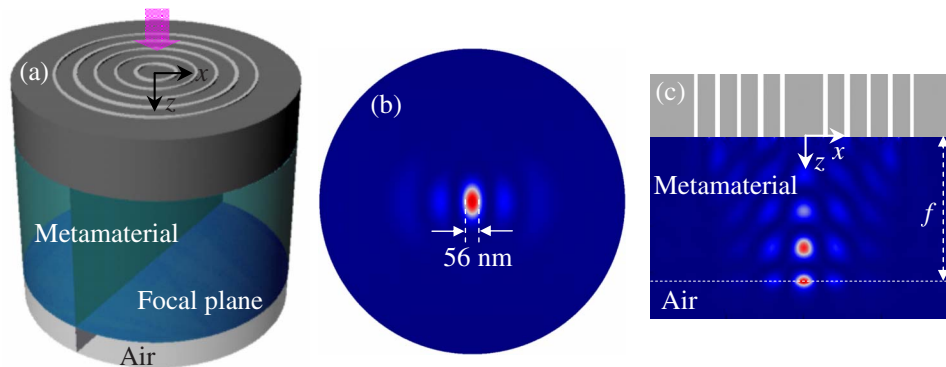


FIG. 4. (Color online) Demonstration of a 3D metalens with truncated metamaterial at its focal length. (a) Schematic geometry. Profile of  $|E_x|^2$  at (b) the horizontal plane 10 nm below the focal plane and (c) the vertical  $xz$  plane. Designed focal length  $f=0.5 \mu\text{m}$ , illuminated by a normal plane wave with the electric field polarization in the  $x$  direction. Metamaterial properties:  $(\epsilon_{xy}=3.4-0.05i, \epsilon_z=11.3-0.9i)$ . Material in slits: air. Metalens dimensions: diameter  $=1.0 \mu\text{m}$  and height  $=0.7 \mu\text{m}$ . PWC height:  $0.2 \mu\text{m}$ . Slit widths: 10–20 nm.

2(d). This rather counterintuitive behavior comes from the negative refraction experienced at the interface between a hyperbolically dispersive metamaterial and a common medium, and drastically diversifies the functionalities of the lens and thus optical systems.

A metalens is also expected to be able to focus a cylindrical wave directly into an image under specific condition as a conventional lens does. Figure 3 shows such an example. An object in air can form its image in the metamaterials at a location between  $f$  and  $2f$  [see Fig. 3(a)], where  $f$  is the focal length in metamaterial. When the object is 400 nm off the optical axis in air, the image is shifted by 86 nm, attaining a demagnification of 4.65, as shown in Fig. 3(b). This behavior is consistent with the case of conventional lenses; when an image is formed between  $f$  and  $2f$ , it is always minified. The image resolution however is in deep subwavelength scale in the metamaterial due to its extraordinary material properties. It is no surprise that when an object is placed between  $f$  and  $2f$ , a magnified image will be formed, as shown in Figs. 3(c) and 3(d). All of these metalens properties can be fully engineered for a specific application using a procedure similar to the conventional lens design.

The metalens concept can be easily extended to three dimension (3D) for realistic applications. Figure 4 shows the schematic geometry and simulations for a 3D metalens with its metamaterial truncated at its focal plane. This 3D metalens consists of an Ag PWC with five annular slits and a metamaterial slab with an elliptic dispersion. The metalens is illuminated with a linearly  $x$ -polarized normal plane wave. Figures 4(b) and 4(c) show the simulated  $|E_x|^2$  profiles at a horizontal plane 10 nm below the focal plane and the vertical  $xz$  plane, respectively. Figure 4(c) shows that the near field at the bottom surface of the metalens in air can be directly accessed and utilized. Therefore, such a metalens may be used for imaging, sensing, lithography, and optical storage purposes with super resolution.

We want to emphasize that all the metamaterials properties used in the above demonstrations are real values based on effective media estimation in metal/dielectric multilayer composites<sup>23</sup> and metallic nanowires in dielectric matrix.<sup>24</sup> The metalens concept can be extended to other light frequencies, electromagnetic waves, and even acoustic waves, etc. Similar to the microlens array<sup>25</sup> or zone plate array system,<sup>26</sup> an array of metalenses can be assembled for large area processing.

In summary, we have proposed and demonstrated a metalens concept by using the combination of a nonperiodic PWC and a metamaterial slab. The metalens behaves similar but more omnipotent than a conventional optical lens. The simulation results confirms that the metalens has Fourier transform, deep subwavelength focusing, and imaging capabilities.

- <sup>1</sup>E. Abbe, *Arch. Mikroskop. Anat.* **9**, 413 (1873).
- <sup>2</sup>S. M. Mansfield and G. S. Kino, *Appl. Phys. Lett.* **57**, 2615 (1990).
- <sup>3</sup>B. D. Terris, H. J. Mamin, D. Rugar, W. R. Studenmund, and G. S. Kino, *Appl. Phys. Lett.* **65**, 388 (1994).
- <sup>4</sup>Q. Wu, G. D. Feke, R. D. Grober, and L. P. Ghislain, *Appl. Phys. Lett.* **75**, 4064 (1999).
- <sup>5</sup>J. B. Pendry, *Phys. Rev. Lett.* **85**, 3966 (2000).
- <sup>6</sup>N. Fang, H. Lee, C. Sun, and X. Zhang, *Science* **308**, 534 (2005).
- <sup>7</sup>A. Salandrino and N. Engheta, *Phys. Rev. B* **74**, 075103 (2006).
- <sup>8</sup>T. Taubner, D. Korobkin, Y. Urzhumov, G. Shvets, and R. Hillenbrand, *Science* **313**, 1595 (2006).
- <sup>9</sup>Z. Jacob, L. V. Alekseyev, and E. Narimanov, *Opt. Express* **14**, 8247 (2006).
- <sup>10</sup>I. I. Smolyaninov, Y. J. Hung, and C. C. Davis, *Science* **315**, 1699 (2007).
- <sup>11</sup>Z. Liu, H. Lee, Y. Xiong, C. Sun, and X. Zhang, *Science* **315**, 1686 (2007).
- <sup>12</sup>Z. Liu, S. Durant, H. Lee, Y. Pikus, N. Fang, Y. Xiong, C. Sun, and X. Zhang, *Nano Lett.* **7**, 403 (2007).
- <sup>13</sup>X. Zhang and Z. Liu, *Nat. Mater.* **7**, 435 (2008).
- <sup>14</sup>D. R. Smith, J. B. Pendry, and M. C. K. Wiltshire, *Science* **305**, 788 (2004).
- <sup>15</sup>V. M. Shalaev, *Nat. Photonics* **1**, 41 (2007).
- <sup>16</sup>J. Yao, Z. Liu, Y. Liu, Y. Wang, C. Sun, G. Bartal, A. M. Stacy, and X. Zhang, *Science* **321**, 930 (2008).
- <sup>17</sup>C. G. Parazzoli, R. B. Greeger, J. A. Nielsen, M. A. Thompson, K. Li, A. M. Vetter, M. H. Tanielian, and D. C. Vier, *Appl. Phys. Lett.* **84**, 3232 (2004).
- <sup>18</sup>C. Ma and Z. Liu, *Opt. Express* **18**, 4838 (2010).
- <sup>19</sup>H. Shi, C. Wang, C. Du, X. Luo, X. Dong, and H. Gao, *Opt. Express* **13**, 6815 (2005).
- <sup>20</sup>L. Verslegers, P. B. Catrysse, Z. Yu, J. S. White, E. S. Barnard, M. L. Brongersma, and S. Fan, *Nano Lett.* **9**, 235 (2009).
- <sup>21</sup>Z. Sun and H. K. Kim, *Appl. Phys. Lett.* **85**, 642 (2004).
- <sup>22</sup>J. A. Dionne, L. A. Sweatlock, H. A. Atwater, and A. Polman, *Phys. Rev. B* **73**, 035407 (2006).
- <sup>23</sup>S. Anantha Ramakrishna, J. B. Pendry, M. C. K. Wiltshire, and W. J. Stewart, *J. Mod. Opt.* **50**, 1419 (2003).
- <sup>24</sup>J. B. Pendry, A. J. Holden, D. J. Robbins, and W. J. Stewart, *J. Phys.: Condens. Matter* **10**, 4785 (1998).
- <sup>25</sup>R. Völkel, H. P. Herzig, P. Nussbaum, R. Dandliker, and W. B. Hügler, *Opt. Eng. (Bellingham)* **35**, 3323 (1996).
- <sup>26</sup>H. I. Smith, R. Menon, A. Patel, D. Chao, M. Walsh, and G. Barbastathis, *Microelectron. Eng.* **83**, 956 (2006).